

Exploring Chromium(III)–Alkyl Bond Homolysis with CpCr[(ArNCMe)₂CH](R) Complexes

K. Cory MacLeod,[†] Julia L. Conway,[†] Brian O. Patrick,[‡] and Kevin M. Smith*[†]

Department of Chemistry, University of British Columbia Okanagan, 3333 University Way, Kelowna, BC, Canada V1V 1V7, and Department of Chemistry, University of British Columbia, Vancouver, British Columbia, Canada V6T 1Z1

Received September 15, 2010; E-mail: kevin.m.smith@ubc.ca

Abstract: A range of paramagnetic Cr(III) monohydrocarbyl complexes CpCr[(ArNCMe)₂CH](R) (Ar = *ortho*-disubstituted aryl; R = primary alkyl, trimethylsilylmethyl, benzyl, phenyl, alkenyl, or alkynyl) were synthesized to investigate how varying the steric and electronic properties of the R group affected their propensity for Cr–R bond homolysis. Most complexes were prepared by salt metathesis of known CpCr[(ArNCMe)₂CH](Cl) compounds in Et₂O with commercial RMgCl solutions, although more sterically demanding combinations of Ar and R groups necessitated the use of halide-free MgR₂ reagents and the Cr(III) tosylate or triflate derivatives. Alternative synthetic routes to Cr(III)–R species using the previously reported Cr(II) compounds CpCr[(ArNCMe)₂CH] and sources of R• radicals (e.g., BEt₃ and air) were also explored. The UV–vis spectra of the CpCr[(ArNCMe)₂CH](R) complexes possessed two strong bands with maximum absorbances in the ranges 395–436 nm and 535–582 nm, with the band in the latter range being particularly characteristic of the Cr(III)–R compounds. The Cr–CH₂R bond lengths as determined by single-crystal X-ray diffraction were longer than those in the corresponding Cr–CH₃ complexes, typically falling in the range 2.10 to 2.13 Å. The Cr(III) benzyl compounds displayed longer Cr–CH₂Ph distances, while the bond lengths for the alkenyl and alkynyl species were substantially shorter. The rate of Cr–R bond homolysis at room temperature was determined by monitoring the reaction of Cr(III) neopentyl, benzyl, and isobutyl complexes with excess PhSSPh using UV–vis spectroscopy. Although the other primary alkyl, phenyl, and alkenyl compounds did not undergo appreciable homolysis under these conditions, they were cleanly converted to CpCr[(ArNCMe)₂CH](SPh) by photolysis.

Introduction

Alkyl complexes of first-row transition metals have gained increasing prominence in catalytic carbon–carbon bond forming reactions. In cross-coupling reactions involving alkyl halide substrates, catalysts based on cobalt, nickel, and iron display reactivity complementary to established palladium systems.¹ It has become increasingly apparent that metal–alkyl bond homolysis to form carbon-based radicals is a critical step in many of these successful new catalytic cycles.¹ Reversible M–R homolysis has long been recognized as a characteristic reactivity mode for Co(III)–alkyl complexes,² and cobalt reagents have been employed to control radical reactivity as stoichiometric reagents³ and as catalysts⁴ for organic synthesis. However, reversible metal–alkyl bond homolysis has also been demon-

strated by Vicić,⁵ Hu,⁶ and Cárdenas⁷ in nickel-based cross-coupling catalysts. Somewhat counterintuitively, it is the intermediacy of radicals that permit the enantioselective conversion of racemic organic halides to chiral products in Fu's cross-coupling reactions with chiral nickel catalysts.⁸ Even in iron systems, the reaction of Fe(II) with organic radicals to generate Fe(III) and carbon-based radicals has been proposed as a key feature of catalytic C–C bond forming reactions^{9,10} and as a means to shuttle between Fe(II)/Fe(0) and Fe(III)/Fe(I) redox couples.¹¹

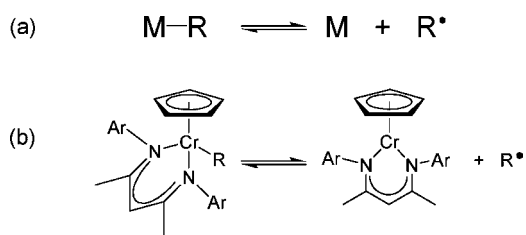
[†] University of British Columbia Okanagan.

[‡] University of British Columbia, Vancouver.

- (1) Rudolph, A.; Lautens, M. *Angew. Chem., Int. Ed.* **2009**, *48*, 2656–2670.
- (2) (a) Halpern, J. *Polyhedron* **1988**, *7*, 1483–1490. (b) Pattenden, G. *Chem. Soc. Rev.* **1988**, *17*, 361–382.
- (3) (a) Branchaud, B. P.; Meier, M. S.; Malekzadeh, M. N. *J. Org. Chem.* **1987**, *52*, 212–217. (b) Ali, A.; Gill, G. B.; Pattenden, G.; Roan, G. A.; Kam, T.-S. *J. Chem. Soc., Perkin Trans. 1* **1996**, 1081–1093.
- (4) (a) Affo, W.; Ohmiya, H.; Fujioka, T.; Ikeda, Y.; Nakamura, T.; Yorimitsu, H.; Oshima, K.; Imamura, Y.; Mizuta, T.; Miyoshi, K. *J. Am. Chem. Soc.* **2006**, *128*, 8068–8077. (b) Waser, J.; Gaspar, B.; Nambu, H.; Carreira, E. M. *J. Am. Chem. Soc.* **2006**, *128*, 11693–11712.

- (5) Jones, G. D.; Martin, J. L.; McFarland, C.; Allen, O. R.; Hall, R. E.; Haley, A. D.; Brandon, R. J.; Konovalova, T.; Desrochers, P. J.; Pulay, P.; Vicić, D. A. *J. Am. Chem. Soc.* **2006**, *128*, 13175–13183.
- (6) Vechorkin, O.; Proust, V.; Hu, X. *J. Am. Chem. Soc.* **2009**, *131*, 9756–9766.
- (7) Phapale, V. B.; Buñuel, E.; García-Iglesias, M.; Cárdenas, D. J. *Angew. Chem., Int. Ed.* **2007**, *46*, 8790–8795.
- (8) Lundin, P. M.; Fu, G. C. *J. Am. Chem. Soc.* **2010**, *132*, 11027–11029, and references cited therein.
- (9) (a) Noda, D.; Sunada, Y.; Hatakeyama, T.; Nakamura, M.; Nagashima, H. *J. Am. Chem. Soc.* **2009**, *131*, 6078–6079. (b) Hatakeyama, T.; Hashimoto, T.; Kondo, Y.; Fujiwara, Y.; Seike, H.; Takaya, H.; Tamada, Y.; Ono, T.; Nakamura, M. *J. Am. Chem. Soc.* **2010**, *132*, 10674–10676.
- (10) Vallée, F.; Mousseau, J. J.; Charette, A. B. *J. Am. Chem. Soc.* **2010**, *132*, 1514–1516.
- (11) Fürstner, A.; Martin, R.; Krause, H.; Seidel, G.; Goddard, R.; Lehmann, C. W. *J. Am. Chem. Soc.* **2008**, *130*, 8773–8787.

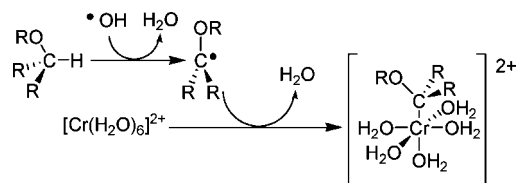
Scheme 1. Reversible Metal–Alkyl Bond Homolysis



The ability of metal alkyl complexes to both generate and trap carbon-based radicals is also the foundation of organometallic-mediated radical polymerization (OMRP),¹² where the low concentration of R^\bullet in solution is maintained by the equilibrium shown in Scheme 1a. Although first developed for cobalt reagents,¹³ OMRP has since been demonstrated using other first-row transition metals including iron¹⁴ and vanadium.¹⁵ We recently reported the use of a well-defined Cr(III) alkyl complex to control the radical polymerization of vinyl acetate.¹⁶ The effectiveness of the OMRP reagent was found to depend on the identity of the alkyl group. The methyl complex, $\text{CpCr}[(\text{XylNCMe})_2\text{CH}](\text{CH}_3)$ (**1**) (Xyl = xylyl, 2,6- $\text{Me}_2\text{C}_6\text{H}_3$), that we had previously synthesized in the investigation of the single-electron oxidative addition of iodomethane with $\text{CpCr}[(\text{XylNCMe})_2\text{CH}]$ ¹⁷ was found to generate only small amounts of poly(vinyl acetate) with poor polydispersity after 48 h in neat vinyl acetate at room temp. In contrast, the corresponding neopentyl complex $\text{CpCr}[(\text{XylNCMe})_2\text{CH}](\text{CH}_2\text{CMe}_3)$ (**2**) served both to initiate and to control the radical polymerization of vinyl acetate.¹⁶

These observations are consistent with previously established organochromium chemistry.¹⁸ The ability of aqueous Cr(II) to trap carbon-based radicals was demonstrated over half a century ago with the preparation of $[(\text{H}_2\text{O})_5\text{Cr}(\text{CH}_2\text{Ph})]^{2+}$ _(aq).¹⁹ Initially synthesized by single-electron oxidative addition of Cr(II) with benzyl chloride, a wider range of Cr(III) alkyl species can be prepared *in situ* via the radical C–H bond activation process shown in Scheme 2. Mixtures of Cr(II)_(aq) and an excess of the organic substrate are treated with hydroxyl radicals, generated by the reaction of Cr(II)_(aq) with added H_2O_2 ²⁰ or by pulse radiolysis.²¹ The reactive $\cdot\text{OH}$ radical abstracts H^\bullet from the ether or alcohol, and rapid trapping of the resulting organic radical with Cr(II) forms the observed $[(\text{H}_2\text{O})_5\text{Cr}(\text{CR}_2(\text{OR}))]^{2+}$ _(aq) species. The rate of trapping of R^\bullet by Cr(II)_(aq) is close to the diffusion control limit at 2×10^7 to $3 \times 10^8 \text{ M}^{-1} \text{ s}^{-1}$ and is

Scheme 2. Synthesis of Aqueous Cr(III) Alkyl Compounds via Radical C–H Activation



relatively invariant with the identity of the organic radical.²² High-pressure kinetic studies indicated that the radical trapping rate is hindered by dissociation of H_2O from the $[\text{Cr}(\text{H}_2\text{O})_6]^{2+}$ dication,²² even though water exchange in $\text{Cr}(\text{II})_{(\text{aq})}$ is among the very fastest rates for any $[\text{M}(\text{H}_2\text{O})_n]^{m+}$ aqueous transition metal complex.²³ The efficient trapping of R^\bullet by Cr(II) also underpins the Cr-mediated coupling of organic halides and aldehydes.²⁴ The reaction of Cr(II) and R^\bullet is only rendered reversible through adverse steric interactions and/or significant electronic stabilization of the resulting organic radical.^{20,25}

We are interested in using well-defined Cr(III) alkyl complexes for controlling radical intermolecular C–C bond forming reactions, both for OMRP and for synthetic organic applications. Understanding how varying the identity of the alkyl group influences its propensity for homolytic Cr–R bond cleavage would aid in the design of these reagents. The $\text{CpCr}[(\text{ArNCMe})_2\text{CH}](\text{R})$ system possesses several attractive features for this type of investigation (Scheme 1b). The β -diketiminate ligand can be systematically modified,²⁶ and the resulting Cr(III) alkyl complexes are readily recrystallized from hexanes. The high spin d^4 , Cr(II) complexes $\text{CpCr}[(\text{ArNCMe})_2\text{CH}]$ can be independently synthesized;^{17,27,28} are monomeric and stable as solids and in solution under anhydrous, anaerobic conditions; and are coordinatively unsaturated. The latter factor ensures that no ligand dissociation is required prior to radical trapping, unlike some Co(II) complexes²⁹ or the Cr(II)_(aq) species mentioned above.²² Computational studies indicate that the barrier for Cr(III)–R formation from $\text{CpCr}[(\text{ArNCMe})_2\text{CH}]$ and alkyl radicals is only $\sim 1 \text{ kcal/mol}$.¹⁶ The use of monoalkyl Cr(III) complexes also avoids complications due to intramolecular alkyl group reactivity observed for known bis- or tris-alkyl Cr(III) systems. For instance, Sneed noted that the trend for thermal stabilities of $\text{CrR}_3(\text{THF})_n$ complexes (aryl > allyl > benzyl > alkyl > alkenyl) did not correlate with the relative stabilities of the corresponding organic radicals.¹⁸ Similarly, $\text{Cp}^*\text{Cr}(\text{L})(\text{R})_2$

(12) (a) Poli, R. *Angew. Chem., Int. Ed.* **2006**, *45*, 5058–5070. (b) Smith, K. M.; McNeil, W. S.; Abd-El-Aziz, A. S. *Macromol. Chem. Phys.* **2010**, *211*, 10–16. (c) di Lena, F.; Matyjaszewski, K. *Prog. Polym. Sci.* **2010**, *35*, 959–1021.

(13) Debuigne, A.; Poli, R.; Jérôme, C.; Jérôme, R.; Detrembleur, C. *Prog. Polym. Sci.* **2009**, *34*, 211–239.

(14) Shaver, M. P.; Allan, L. E. N.; Rzepa, H. S.; Gibson, V. C. *Angew. Chem., Int. Ed.* **2006**, *45*, 1241–1244.

(15) Shaver, M. P.; Hanhan, M. E.; Jones, M. R. *Chem. Commun.* **2010**, *46*, 2127–2129.

(16) Champouret, Y.; MacLeod, K. C.; Baisch, U.; Patrick, B. O.; Smith, K. M.; Poli, R. *Organometallics* **2010**, *29*, 167–176.

(17) MacLeod, K. C.; Conway, J. L.; Tang, L.; Smith, J. J.; Corcoran, L. D.; Ballem, K. H. D.; Patrick, B. O.; Smith, K. M. *Organometallics* **2009**, *28*, 6798–6806.

(18) Sneed, R. P. A. *Organochromium Compounds*; Academic Press: New York, 1975.

(19) (a) Anet, F. A. L.; Leblanc, E. *J. Am. Chem. Soc.* **1957**, *79*, 2649–2650. (b) Anet, F. A. L. *Can. J. Chem.* **1959**, *37*, 58–61. (c) Smith, K. M. *Coord. Chem. Rev.* **2006**, *250*, 1023–1031.

(20) Espenson, J. H. *Prog. Inorg. Chem.* **1983**, *30*, 189–212.

(21) van Eldik, R.; Meyerstein, D. *Acc. Chem. Res.* **2000**, *33*, 207–214.

(22) van Eldik, R.; Gaede, W.; Cohen, H.; Meyerstein, D. *Inorg. Chem.* **1992**, *31*, 3695–3696.

(23) Helm, L.; Merbach, A. E. *Chem. Rev.* **2005**, *105*, 1923–1959.

(24) (a) Fürstner, A. *Chem. Rev.* **1999**, *99*, 991–1045. (b) Guo, H.; Dong, C.; Kim, D.; Urabe, D.; Wang, J.; Kim, J. T.; Liu, X.; Sasaki, T.; Kishi, Y. *J. Am. Chem. Soc.* **2009**, *131*, 15387–15393.

(25) (a) Takai, K.; Matsukawa, N.; Takahashi, A.; Fujii, T. *Angew. Chem., Int. Ed.* **1998**, *37*, 152–155. (b) Wessjohann, L. A.; Schmidt, G.; Schrekker, H. S. *Tetrahedron* **2008**, *64*, 2134–2142.

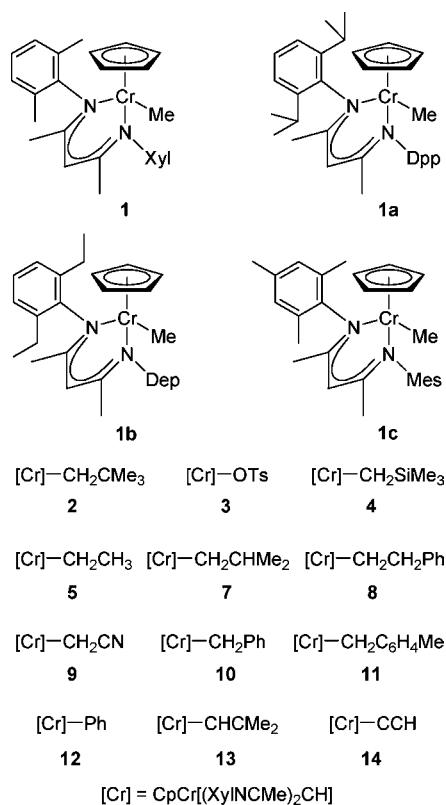
(26) (a) Bourget-Merle, L.; Lappert, M. F.; Severn, J. R. *Chem. Rev.* **2002**, *102*, 3031–3065. (b) Mindiola, D. J. *Angew. Chem., Int. Ed.* **2009**, *48*, 6198–6200.

(27) Doherty, J. C.; Ballem, K. H. D.; Patrick, B. O.; Smith, K. M. *Organometallics* **2004**, *23*, 1487–1489.

(28) Champouret, Y.; Baisch, U.; Poli, R.; Tang, L.; Conway, J. L.; Smith, K. M. *Angew. Chem., Int. Ed.* **2008**, *47*, 6069–6072.

(29) Maria, S.; Kaneyoshi, H.; Matyjaszewski, K.; Poli, R. *Chem.—Eur. J.* **2007**, *13*, 2480–2492.

Chart 1



complexes display distinct decomposition modes depending on the alkyl substituent for R = allyl,³⁰ benzyl,³¹ or trimethylsilylmethyl.³²

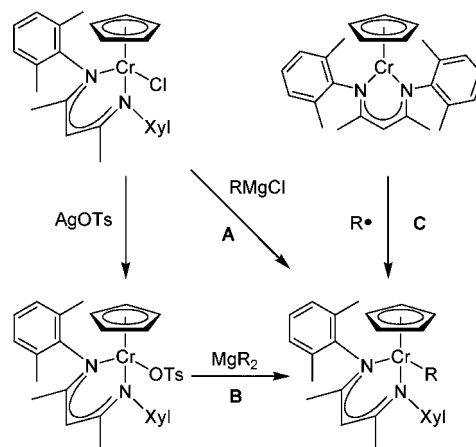
In this paper, we report the synthesis of the CpCr[(XylNCMe)₂CH](R) complexes shown in Chart 1. The structures of all of these complexes were confirmed by single crystal X-ray diffraction (see Supporting Information for crystallographic details). For specific alkyl complexes, we have also prepared the analogous compounds bearing β-diketimate ligands with alternative N-aryl substituents. In this paper, these variants will be designated as shown in Chart 1 for the previously reported CpCr[(ArNCMe)₂CH](Me) complexes: **1a**, Ar = Dpp (2,6-diisopropylphenyl, 2,6-(Me₂CH)₂C₆H₃); **1b**, Ar = Dep (2,6-diethylphenyl, 2,6-(CH₃CH₂)₂C₆H₃); **1c**, Ar = Mes (mesityl, 2,4,6-Me₃C₆H₂).^{17,27} The reaction of these complexes with excess PhSSPh was monitored using UV–visible spectroscopy, permitting the determination of the Cr(III)–R homolysis rates for the more reactive neopentyl and benzyl compounds. Although no thermal homolysis was measured for most of the remaining complexes at ambient temperature, the presence of excess PhSSPh revealed photolytic reactivity that we had not previously appreciated.

Results and Discussion

Synthetic Routes to CpCr[(ArNCMe)₂CH](R) Complexes.

The new CpCr[(DppNCMe)₂CH](R) compounds (R = CH₂SiMe₃ (**4a**), CH₂CHMe₂ (**7a**), and CH₂Ph (**10a**)) were

Scheme 3. Synthetic Routes to Cr(III)–R Compounds



prepared from the Cr(III) triflate derivative, as previously reported for Cr(III) methyl complex **1a**.²⁷ Both Cr(III) chloride and Cr(III) tosylate precursors were used to prepare CpCr[(ArNCMe)₂CH](R) complexes (Ar = Xyl, Dep, or Mes) by salt metathesis, as shown in Scheme 3. The more convenient route is method **A**: CpCr[(ArNCMe)₂CH](Cl) reacted in Et₂O at room temp with commercial solutions of RMgX, followed by addition of commercial anhydrous 1,4-dioxane, Celite filtration to remove the precipitated MgX₂ salts, and recrystallization of the Cr(III) alkyl products from hexanes at –35 °C. In cases where the desired combination of R and NAr substituents resulted in significant steric congestion, an alternative synthetic approach was employed. The Cr(III) tosylate precursors for method **B** in Scheme 3, **3b** (Ar = Dep) and **3c** (Ar = Mes), were synthesized by treating CpCr[(ArNCMe)₂CH](Cl) with AgOTs as described for **3** (Ar = Xyl)¹⁶ and were air-stable as crystalline solids. In method **B**, Cr(III) tosylate complex **3b**, or **3c** was reacted with halide-free MgR₂ reagents to avoid competing Cr(III)–X formation.³³ For example, although CpCr[(XylNCMe)₂CH](CH₂SiMe₃), **4**, (Figure 1) could be prepared via method **A**, the reaction proceeded to completion more quickly using method **B**.

Method **C** in Scheme 3 takes advantage of the ability of Cr(II) to trap carbon-based radicals. The application of this route to synthesize **4** by reacting CpCr[(XylNCMe)₂CH] with 1.5 equiv

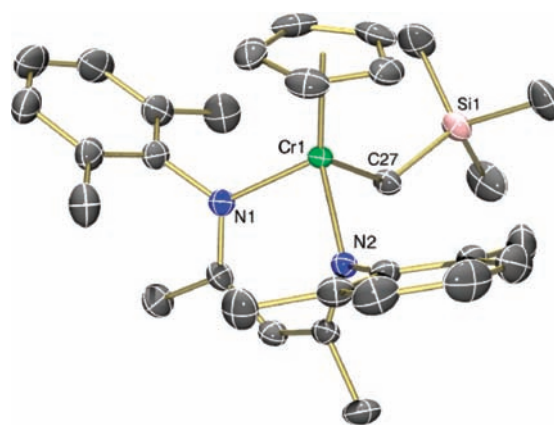
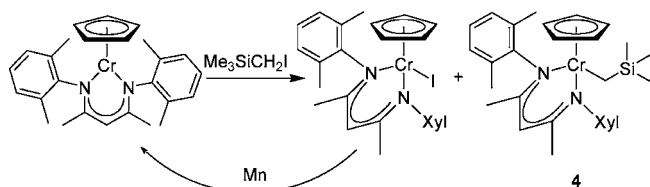


Figure 1. Thermal ellipsoid diagram (50%) of **4**. All H atoms and one half-molecule of hexanes are omitted for clarity.

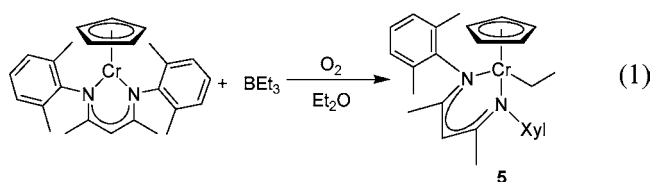
(30) Döhring, A.; Emrich, R.; Goddard, R.; Jolly, P. W.; Krüger, C. *Polyhedron* **1993**, *12*, 2671–2680.

(31) Bhandari, G.; Kim, Y.; McFarland, J. M.; Rheingold, A. L.; Theopold, K. H. *Organometallics* **1995**, *14*, 738–745.

(32) Heintz, R. A.; Leelasubcharoen, S.; Liable-Sands, L. M.; Rheingold, A. L.; Theopold, K. H. *Organometallics* **1998**, *17*, 5477–5485.

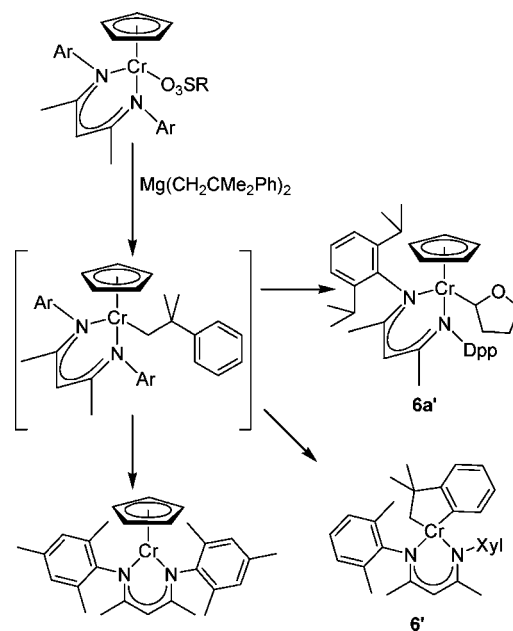
Scheme 4. Synthesis of **4** from R-I and Mn (Method C)

of $\text{Me}_3\text{SiCH}_2\text{I}$ and an excess of Mn is shown in Scheme 4.³⁴ Use of Zn or Mg to reduce the Cr(III) iodide back to the active Cr(II) form did not lead to clean conversion to **4**, as determined by UV–vis spectroscopic analysis of the crude reaction mixtures. Manganese powder has found use as a selective stoichiometric reductant for other reactions of first-row transition metals with organic substrates, from Fürstner's catalytic-inchromium variant of the Nozaki–Hiyama–Kishi reaction³⁵ to more recent work with titanocene³⁶ and nickel³⁷ catalysts.



Another example of method C is the synthesis of $\text{CpCr}[(\text{XylNCMe})_2\text{CH}](\text{CH}_2\text{CH}_3)$ (**5**) shown in eq 1. By UV–vis spectroscopy, there is no apparent reaction between BEt_3 and $\text{CpCr}[(\text{XylNCMe})_2\text{CH}]$ in Et_2O . However, exposure of the dilute reaction mixture to air results in the rapid consumption of Cr(II) and the clean formation of **5**, as determined by comparison of the UV–vis spectrum of an authentic sample prepared via method A. Both trialkylboranes and *B*-alkylcatecholboranes are known to release $\text{R}\cdot$ when treated with O_2 or alkoxy radicals.³⁸ The presence of excess air, BEt_3 , and oxidized boron byproducts renders the reaction in eq 1 unsuitable for isolation of the Cr(III) ethyl complex. However, it does present an intriguing potential method for the *in situ* generation of functionalized Cr(III) alkyl species derived from hydroboration.

Attempted Synthesis of Neophyl Complexes. As noted in our initial 2004 communication, attempts to prepare $\text{CpCr}[(\text{DppNCMe})_2\text{CH}](\text{R})$ complexes more sterically demanding than methyl complex **1a** were unsuccessful.²⁷ Suspecting possible deprotonation of the β -diketiminato ligand,³⁹ we tried the reaction shown in Scheme 5 to identify the major decomposition product. X-ray diffraction of the crystals isolated in

Scheme 5. Attempted Synthesis of Cr(III)– $\text{CH}_2\text{CMe}_2\text{Ph}$ Complexes

low yields from this reaction demonstrated that the product was neither the presumed neophyl intermediate $\text{CpCr}[(\text{DppNCMe})_2\text{CH}](\text{CH}_2\text{CMe}_2\text{Ph})$ (**6a**) nor the direct result of ancillary ligand deprotonation, but rather the product of activation of the THF reaction solvent, **6a'**.⁴⁰ Attempts to prepare the cyclopentyl analog of **6a'**, $\text{CpCr}[(\text{DppNCMe})_2\text{CH}](\text{C}_5\text{H}_9)$, by salt metathesis also gave unanticipated results.⁴¹ Subsequent reactions of Cr(III) tosylate **3** or **3c** with halide-free $\text{Mg}(\text{CH}_2\text{CMe}_2\text{Ph})_2$ reagents also gave very low yields of crystalline products. X-ray diffraction revealed these to be Cp-free metalated $\text{Cr}[(\text{XylNCMe})_2\text{CH}](\text{C}_6\text{H}_4\text{CMe}_2\text{CH}_2)$ (**6'**)⁴² (Figure 2) and the Cr(II) complex $\text{CpCr}[(\text{MesNCMe})_2\text{CH}]$ (Scheme 5). Presumably there is a mixture of compounds formed for all of the reactions with preferential recrystallization resulting in characterization of different complexes as the β -diketiminato ligand is changed. No further attempts were made to optimize the reaction with $\text{Mg}(\text{CH}_2\text{CMe}_2\text{Ph})_2$ to obtain **6** or any one of the other products shown in Scheme 5.

Gratifyingly, only relatively minor variations of the Cr– $\text{CH}_2\text{CMe}_2\text{Ph}$ group were required to produce the desired Cr(III) alkyl complexes. The Dep (**2b**) and Mes (**2c**) substituted neopentyl compounds were prepared by method B, analogous

- (33) (a) Andersen, R. A.; Wilkinson, G. *J. Chem. Soc., Dalton Trans.* **1977**, 809–811. (b) Dryden, N. H.; Legzdins, P.; Trotter, J.; Yee, V. C. *Organometallics* **1991**, *10*, 2857–2870. (c) For a recent synthesis of paramagnetic organomanganese compounds requiring the use of MgR_2 reagents, see: Cámpora, J.; Palma, P.; Pérez, C. M.; Rodríguez-Delgado, A.; Álvarez, E.; Gutiérrez-Puebla, E. *Organometallics* **2010**, *29*, 2960–2970.
- (34) Ogino, H.; Shoji, M.; Abe, Y.; Shimura, M.; Shimoi, M. *Inorg. Chem.* **1987**, *26*, 2542–2546.
- (35) Fürstner, A.; Shi, N. Y. *J. Am. Chem. Soc.* **1996**, *118*, 12349–12357.
- (36) (a) Barrero, A. F.; Herrador, M. M.; Quílez del Moral, J. F.; Arteaga, P.; Akksira, M.; El Hanbali, F.; Arteaga, J. F.; Diéguez, H. R.; Sánchez, E. M. *J. Org. Chem.* **2007**, *72*, 2251–2254. (b) Gansäuer, A.; Fleckhaus, A.; Lafont, M. A.; Okkel, A.; Kotsis, K.; Anoop, A.; Neese, F. *J. Am. Chem. Soc.* **2009**, *131*, 16989–16999. (c) Gansäuer, A.; Shi, L.; Otte, M. *J. Am. Chem. Soc.* **2010**, *132*, 11858–11859.
- (37) (a) Everson, D. A.; Shrestha, R.; Weix, D. J. *J. Am. Chem. Soc.* **2010**, *132*, 920–921. (b) Prinsell, M. R.; Everson, D. A.; Weix, D. J. *Chem. Commun.* **2010**, 46, 5743–5745.
- (38) Ollivier, C.; Renaud, P. *Chem. Rev.* **2001**, *101*, 3415–3434.

- (39) (a) Fekl, U.; Goldberg, K. I. *J. Am. Chem. Soc.* **2002**, *124*, 6804–6805. (b) Basuli, F.; Bailey, B. C.; Watson, L. A.; Tomaszewski, J.; Huffman, J. C.; Mindiola, D. J. *Organometallics* **2005**, *24*, 1886–1906. (c) Bernskoetter, W. H.; Lobkovsky, E.; Chirik, P. J. *Organometallics* **2005**, *24*, 6250–6259. (d) Basuli, F.; Bailey, B. C.; Huffman, J. C.; Mindiola, D. J. *Organometallics* **2005**, *24*, 3321–3334. (e) Eckert, N. A.; Vaddadi, S.; Stoian, S.; Lachicotte, R. J.; Cundari, T. R.; Holland, P. L. *Angew. Chem., Int. Ed.* **2006**, *45*, 6868–6871. (f) Badiei, Y. M.; Dinescu, A.; Dai, X.; Palomino, R. M.; Heinemann, F. W.; Cundari, T. R.; Warren, T. H. *Angew. Chem., Int. Ed.* **2008**, *47*, 9961–9964. (g) Adhikari, K.; Basuli, F.; Orlando, J. H.; Gao, X.; Huffman, J. C.; Pink, M.; Mindiola, D. J. *Organometallics* **2009**, *28*, 4115–4125.
- (40) Akindele, T.; Yamada, K.; Tomioka, K. *Acc. Chem. Res.* **2009**, *42*, 345–355.
- (41) Ballem, K. H. D.; Smith, K. M.; Patrick, B. O. *Acta Crystallogr.* **2004**, *E60*, m408–m409.
- (42) (a) Carmona, E.; Gutiérrez-Puebla, E.; Marín, J. M.; Monge, A.; Paneque, M.; Poveda, M. L.; Ruiz, C. *J. Am. Chem. Soc.* **1989**, *111*, 2883–2891. (b) Hao, S. K.; Song, J.-I.; Berno, P.; Gambarotta, S. *Organometallics* **1994**, *13*, 1326–1335.

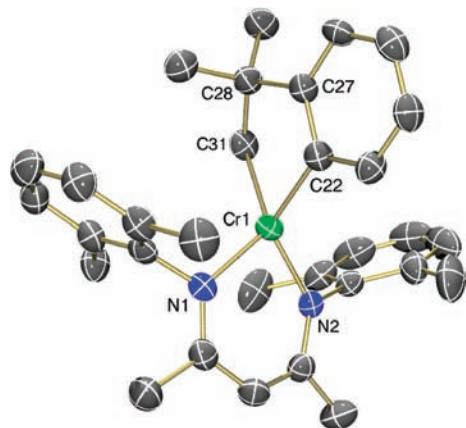


Figure 2. Thermal ellipsoid diagram (50%) of **6'**. Compound **6'** has two independent molecules in the crystal lattice; only one is shown, and all H atoms are omitted for clarity.

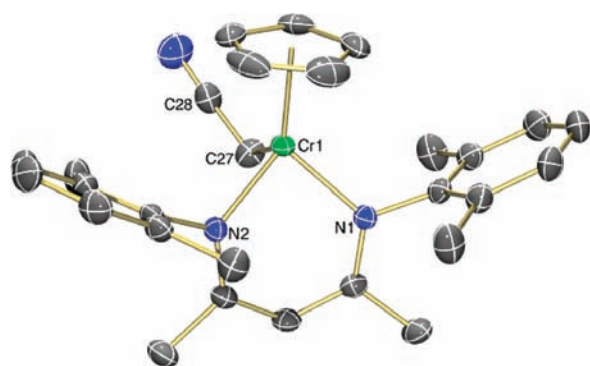


Figure 3. Thermal ellipsoid diagram (50%) of **9**. All H atoms are omitted for clarity.

to the recent synthesis of **2**.¹⁶ Although attempts to prepare the Dpp neopentyl complex also led only to reduction to Cr(II), the corresponding isobutyl compound CpCr[(DppNCMe)₂CH](CH₂CHMe₂) (**7a**) could be isolated via method **B**. For the Xyl β -diketiminato ligand, method **A** was used to prepare isobutyl **7** and phenethyl **8**. Replacing the phenyl and/or methyl substituents of the neophyl ligand with β -hydrogens thus appears to *improve* the stability of the Cr(III) alkyl complexes. This not only underscores the characteristic reluctance of paramagnetic Cr(III) complexes to engage in β -hydrogen elimination reactions^{18,43} but also indicates the high degree of steric discrimination of the CpCr[(ArNCMe)₂CH] system.¹⁶

Electronic Effects: Cyanomethyl and Benzyl. Although adverse steric interactions are undoubtedly involved in the homolysis of Cr(III)–alkyl bonds, we also wished to investigate alkyl group electronic effects. The cyanomethyl compound CpCr[(XylNCMe)₂CH](CH₂CN) (**9**) was readily prepared from the Cr(III) chloride precursor and *in situ* generated KCH₂CN.⁴⁴ As shown in Figure 3, the CH₂CN ligand is C-bound to the Cr as a cyanomethyl⁴⁵ and does not bind through the heteroatom as a ketenimine.⁴⁶ This contrasts with the recently reported enolate complex CpCr[(XylNCMe)₂CH][OC(Ph)CH₂], which was found to bond to Cr through the oxygen atom.⁴⁷

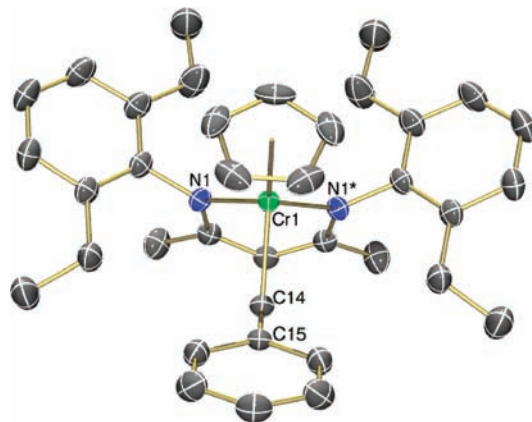


Figure 4. Thermal ellipsoid diagram (50%) of **10b**. All H atoms are omitted for clarity.

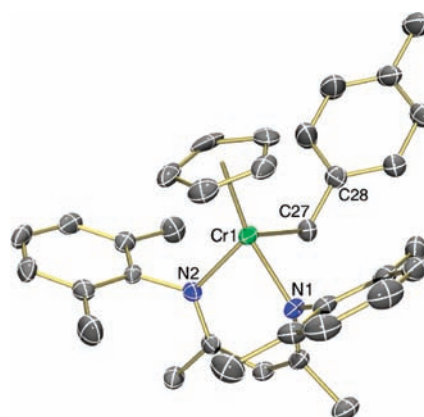


Figure 5. Thermal ellipsoid diagram (50%) of **11**. All H atoms are omitted for clarity.

The benzyl complexes CpCr[(ArNCMe)₂CH](CH₂Ph) (Ar = Xyl (**10**), Dpp (**10a**), Dep (**10b**), and Mes (**10c**)) were prepared by method **A** (**10**, **10b**, **10c**) or from the Cr(III) triflate precursor for **10a**. The X-ray structure of complex **10b** is shown in Figure 4. For both cyanomethyl and benzyl ligands, the substituents stabilize the \cdot CH₂CN and \cdot CH₂Ph radicals, respectively, which should result in a weaker Cr–R bond.^{12a} For instance, primary alkyl [Cr–CH₂R]²⁺_(aq) species do not undergo homolysis, while benzylic [Cr–CH₂Ph]²⁺_(aq) do.⁴⁸

Synthesis via Solvent C–H Atom Abstraction. The Cr–neopentyl derivative **2** was found to convert cleanly to the Cr–benzyl derivative **10** when dissolved in toluene. A similar reaction was observed when **2** was dissolved in a 10:1 mixture of benzene/*p*-xylene to yield CpCr[(XylNCMe)₂CH](CH₂C₆H₄Me) (**11**) as determined by X-ray diffraction (Figure 5). The observed product of the reaction suggested a radical mechanism by which **2** underwent Cr–C bond homolysis to generate a neopentyl radical, followed by hydrogen atom abstraction from the *p*-xylene to generate a \cdot CH₂C₆H₄Me radical that could then be trapped by CpCr[(XylNCMe)₂CH], as shown in Scheme 6. The observed intramolecular (**10**) and intermo-

(43) Theopold, K. H. *Acc. Chem. Res.* **1990**, *23*, 263–270.

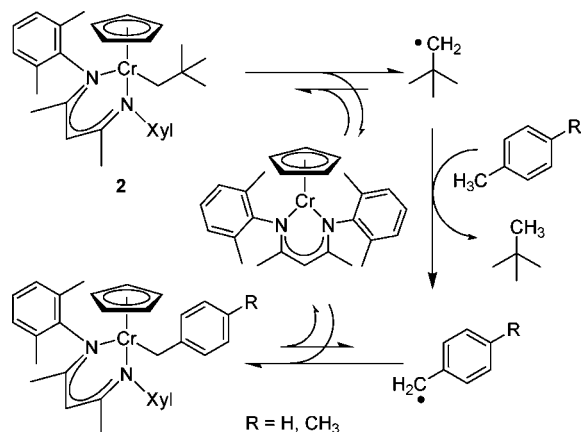
(44) Culkun, D. A.; Hartwig, J. F. *Acc. Chem. Res.* **2003**, *36*, 234–245.

(45) (a) Huber, T. A.; Macartney, D. H.; Baird, M. C. *Organometallics* **1995**, *14*, 592–602. (b) Derrah, E. J.; Giesbrecht, K. E.; McDonald, R.; Rosenberg, L. *Organometallics* **2008**, *27*, 5025–5032.

(46) (a) Fulton, J. R.; Sklenak, S.; Bouwkamp, M. W.; Bergman, R. G. *J. Am. Chem. Soc.* **2002**, *124*, 4722–4737. (b) Oertel, A. M.; Ritleng, V.; Chetcuti, M. J.; Veiros, L. F. *J. Am. Chem. Soc.* **2010**, *132*, 13588–13589.

(47) Champouret, Y.; MacLeod, K. C.; Smith, K. M.; Patrick, B. O.; Poli, R. *Organometallics* **2010**, *29*, 3125–3132.

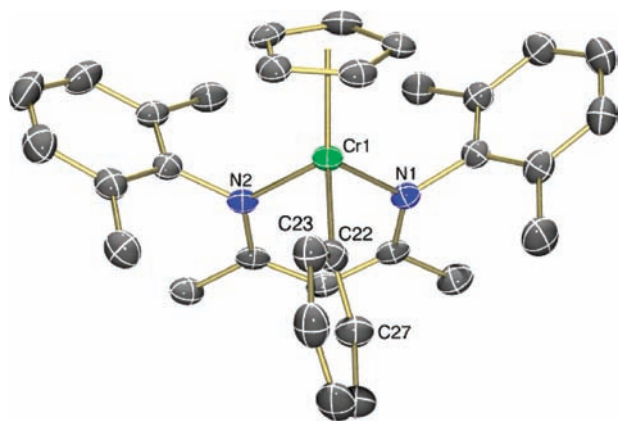
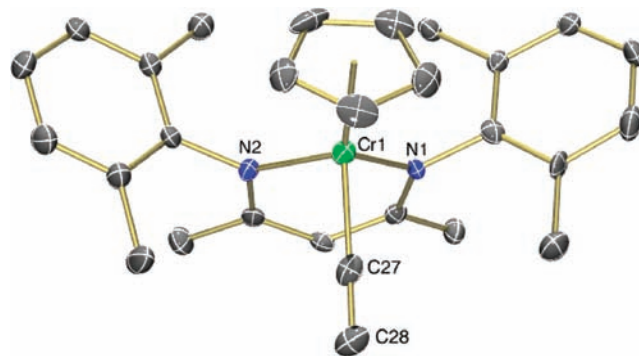
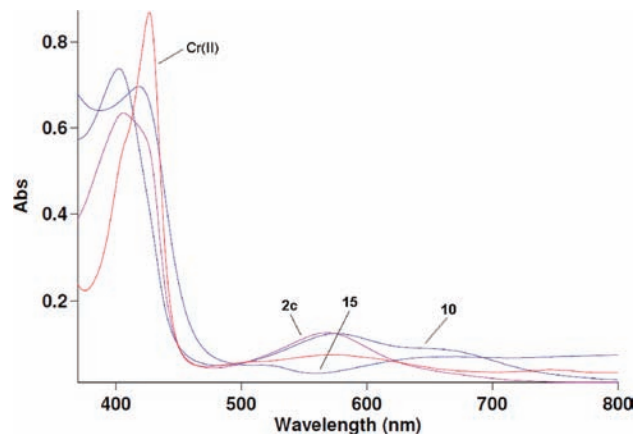
(48) Espenson, J. H. *Acc. Chem. Res.* **1992**, *25*, 222–227.

Scheme 6. Reaction of **2** in Toluene or *p*-Xylene To Produce **10** or **11**

lecular (**11**) selectivity for benzylic over aromatic C–H bond activation is consistent with the trend in C–H bond dissociation energies of H–CH₂Ph < H–CH₂CMe₃ < H–Ph.^{49,50} A similar radical solvent C–H activation mechanism may be operative in the generation of complex **6a'**, discussed above. In these reactions, the reactive •CH₂CMe₂R (R = Me or Ph) radicals serve the same role as observed for the •OH radicals in the synthesis of aqueous Cr(III) alkyl complexes as shown in Scheme 2.

Phenyl, Alkenyl, and Alkynyl Complexes. The Cr(III) phenyl complex CpCr[(Xyl)NCMe₂CH](Ph) (**12**) (Figure 6) was prepared by method **B**. Compound **12** was found to be remarkably stable with no decomposition observed by UV–vis after 4 days at 10^{−4} M in THF or benzene, and it did not initialize polymerization of vinyl acetate at 55 °C after 48 h. The alkenyl complex CpCr[(Xyl)NCMe₂CH](CH=CMe₂) (**13**) and the parent alkynyl complex CpCr[(Xyl)NCMe₂CH](CCH) (**14**) were both prepared by method **A**. The X-ray structure of the Cr–CCH complex is shown in Figure 7.

UV–visible Spectroscopy. All of the CpCr[(Ar)NCMe₂CH]R compounds exhibit two strong absorbance peaks in their UV–vis spectra with λ_{max} in the ranges 395–436 nm and 535–582 nm (Figure 8). The higher energy peak of the phenyl (**12**), alkenyl (**13**), and alkynyl (**14**) compounds is shifted slightly (424–436 nm) compared to the other compounds being reported (395–420 nm). Interestingly, the complexes without Cr–C σ-bonds have peaks in the same ranges but with very different extinction coefficients (ε); the ε values for the Cr(III) chloride,

**Figure 6.** Thermal ellipsoid diagram (50%) of **12**. All H atoms are omitted for clarity.**Figure 7.** Thermal ellipsoid diagram (50%) of **14**. All H atoms are omitted for clarity.**Figure 8.** UV–vis spectra of compounds **2c**, **10**, **15**, and CpCr[(Xyl)NCMe₂CH] at 1.1 × 10^{−4} M in hexanes.

tosylate, and triflate species is larger than the hydrocarbyl compounds for the peak at ~400 nm but is significantly smaller for the lower energy peak at ~550 nm. As a result, UV–visible spectroscopy was invaluable as a preliminary characterization technique for these compounds due to the easily distinguishable spectra of the starting materials and the products of the alkylation reactions.

Although the Cr(III) neopentyl compounds **2b** and **2c** were purified by recrystallization from hexanes, they were found to convert to Cr(II) when diluted to concentrations suitable for UV–vis (10^{−4} M), as previously noted for **2**.¹⁶ The stability of the Cr(III)–R complexes is concentration dependent, since the equilibrium shown in Scheme 1b favors dissociation with dilution. In contrast, UV–vis samples of the other Cr(III)–R compounds in Chart 1 showed no appreciable buildup of Cr(II) during sample preparation.

Notably, small changes in the UV–vis spectra provide a qualitative distinction between many of the compounds due to their differences in color. The Cr(III) chloride, tosylate, and triflate compounds are green to incident light and orange to transmitted light, while many of the Cr(III)–R compounds are purple to both incident and transmitted light. Some exceptions are the Cr(III)–CH₂CN compound which is green to incident and red to transmitted light and the green-blue Cr(III)–CH₂Ph

(49) Blanksby, S. J.; Ellison, G. B. *Acc. Chem. Res.* **2003**, *36*, 255–263.

(50) Nonradical C–H activation reactions with transition-metal complexes usually display a thermodynamic preference for strong C–H bonds; see: Balcells, D.; Clot, E.; Eisenstein, O. *Chem. Rev.* **2010**, *110*, 749–823.

Table 1. Bond Lengths and Angles for CpCr[(ArNCMe)₂CH](R) Complexes

	Ar	R	Cr–C (Å)	Cr–C–E (deg)
2c	Mes	CH ₂ CMe ₃	2.128(2)	134.37(16)
4	Xyl	CH ₂ SiMe ₃	2.0987(14)	131.48(48)
4a	Dpp	CH ₂ SiMe ₃	2.110(2) 2.118(12)	135.71(11) 134.71(11)
4b	Dep	CH ₂ SiMe ₃	2.1098(15)	130.31(8)
4c	Mes	CH ₂ SiMe ₃	2.1031(17)	131.89(9)
5	Xyl	CH ₂ CH ₃	2.090(5) 2.104(5)	127.1(3) 127.4(4)
6a'	Dpp	C ₄ H ₇ O	2.122(4)	122.0(3)
7	Xyl	CH ₂ CHMe ₂	2.121(5) 2.125(5)	126.5(4) 126.6(4)
7a	Dpp	CH ₂ CHMe ₂	2.1269(15) 2.1199(15)	126.15(11) 126.49(11)
8^a	Xyl	CH ₂ CH ₂ Ph	2.200(7) 2.107(7)	114.0(4) 119.6(4)
9	Xyl	CH ₂ CN	2.126(2)	114.67(16)
10	Xyl	CH ₂ Ph	2.1526(15)	121.73(11)
10a	Dpp	CH ₂ Ph	2.1239(13)	126.30(9)
10b	Dep	CH ₂ Ph	2.144(2)	121.63(14)
10c	Mes	CH ₂ Ph	2.1384(19)	120.66(14)
11	Xyl	CH ₂ C ₆ H ₄ Me	2.131(4)	124.3(3)
12	Xyl	Ph	2.098(3)	124.8(3)
13	Xyl	CHCMe ₂	2.050(4) 2.038(4)	142.1(3) 142.4(3)
14	Xyl	CCH	2.009(5)	176.6(5)

^a Compound **8** cocrystallized with CpCr[(XylNCMe)₂CH]Cl.

compounds which have a distinctive shoulder absorbance in their spectra at 650 nm (Figure 8). The Cr(III)–CH₂SiMe₃ compounds are also a slightly different color than the other Cr(III)–R compounds with a violet to transmitted color and the alkenyl and alkynyl analogues which are red and orange-red respectively.

X-ray Crystallography. Single-crystal X-ray diffraction was the preferred method to unambiguously identify each of the paramagnetic CpCr[(ArNCMe)₂CH](R) complexes. We also wished to correlate the observed chromium–alkyl homolysis reactivity described below with any structural changes as the NAr and R groups were modified. For initiation of OMRP of vinyl acetate by CpCr[(XylNCMe)₂CH](R), we had previously noted that the relative efficiency of the methyl (**1**) and neopentyl (**2**) compounds tracked with their Cr–R bond lengths of 2.076(2) Å and 2.136(3) Å, respectively.¹⁶ The Cr–R bond lengths and Cr–C–E (E = C or Si) bond angles for the CpCr[(ArNCMe)₂CH](R) compounds are collected in Table 1, with two sets of values included for compounds that crystallized with two independent molecules in the unit cell. Complete crystallographic information is found in the Supporting Information.

For the CpCr[(ArNCMe)₂CH](R) complexes, the Cr–C bond lengths generally lie in the range 2.10 to 2.13 Å. The Cr–Ph and Cr–CH=CMe₂ bonds are both shorter, at 2.098(3) Å and 2.044(4) (average) Å for **12** and **13**, respectively. At 2.009(5) Å, the CpCr[(XylNCMe)₂CH](CCH) complex has a Cr–alkynyl bond that is shorter than the 2.020(4) Å previously reported for CpCr[(DppNCMe)₂CH](CCPh), consistent with the reduced steric interactions in **14**. The neopentyl complex **2c** lies near the end of the typical range at 2.128(2) Å, which is still shorter than that observed previously for **2**.

The relatively slight variation in the structural parameters for CpCr[(ArNCMe)₂CH](CH₂SiMe₃) as the NAr substituents are modified follow the expected trends. The observed order of Cr–CH₂SiMe₃ bond lengths (**4** < **4c** < **4b** < **4a**) match the increase in steric demand of the Ar groups (Xyl < Mes < Dep

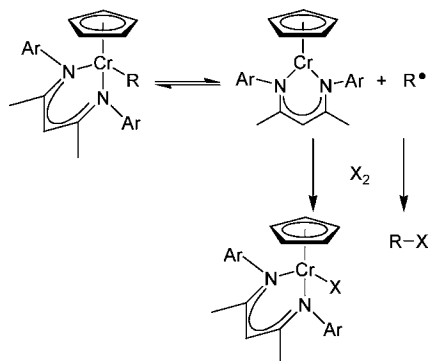
< Dpp). The largest Cr–C–Si angle is also found for **4a**, the complex with the bulkiest Ar substituent. The ethyl complex **5** has a less distorted Cr–C–C angle than **4** but still shows a significantly larger Cr–R distance compared to the corresponding methyl compound **1**. The secondary alkyl complex **6a'** lies well within the 2.10 to 2.13 Å range. The isobutyl compounds **7** and **7a** have relatively long Cr–C bonds, but the Cr–C–C angles are significantly smaller than that of either the neopentyl or trimethylsilylmethyl species, perhaps due to the better fit of the isobutyl group in the cleft defined by the flanking *ortho*-disubstituted NAr groups. The anomalous bond lengths of the phenethyl compound **8** are attributed to the CpCr[(ArNCMe)₂CH]Cl starting material that it cocrystallized with, as has previously been observed for this class of compounds.^{17,47} Although the small Cr–C–C bond angle for **9** indicates that the cyanomethyl group experiences minimal steric hindrance, its Cr–C bond length is much longer than that of ethyl compound **5**, presumably due to the electronic stabilization afforded by the cyano substituent.

The most intriguing bond length trends are those involving the benzyl complexes. The Cr–CH₂Ph bonds are all very long even though their steric constraints are greatly reduced compared to the neopentyl compounds, due to the ability of the flat phenyl substituent to rotate away from the Cp and β-diketiminato ligands. This is consistent with the weaker Cr–CH₂Ph bonds being attributable to the electronic stabilization of the benzylic radical. There is also a large variation in the Cr–C bond lengths as a function of the NAr groups in the CpCr[(ArNCMe)₂CH]-(CH₂Ph) compounds, from 2.1239(13) to 2.1526(15) Å. However, the order of the Cr–C bond lengths (Ar = Dpp **10a** < Mes **10c** < Dep **10b** < Xyl **10**) does not track with the expected steric demands of the *ortho*-disubstituted NAr groups (Xyl ≈ Mes < Dep < Dpp) or match the experimentally determined homolysis rates (**10** ~ **10c** < **10a** ≈ **10b**) as discussed below.

The stretching of the Cr–R bond appears to be a very soft deformation mode for the Cr(III) benzyl complexes, with the observed variations in bond lengths presumably being attributable to crystal packing effects. This matches the previous computational study of bond homolysis of CpCr[(ArNCMe)₂CH]-[CH(Me)OC(O)Me] and its microscopic reverse, trapping R• radicals with CpCr[(ArNCMe)₂CH]. The Cr–C bond lengths at the transition states were calculated to be extremely long at 3.440 and 3.396 Å for Ar = Xyl and Dpp, respectively, consistent with the very low barrier for trapping R• with the Cr(II) compounds.¹⁶ The inherent difficulties in correlating bond lengths from single-crystal X-ray diffraction with observed reactivity trends due to the relative flatness of the potential energy surface for Cr–R bond breaking are reminiscent of the problems faced in assessing structure–activity relationships for Cr–Cr multiple bonds.⁵¹ In each case, the loss of Cr–R or Cr–Cr bonds is compensated by changes in the electronic structure at the chromium center that lower the energy of the unsaturated, high-spin chromium products.⁵² This type of

(51) Horvath, S.; Gorelsky, S. I.; Gambarotta, S.; Korobkov, I. *Angew. Chem., Int. Ed* **2008**, *47*, 9937–9940, and references therein.

(52) Poli, R. *Chem. Rev.* **1996**, *96*, 2135–2204.

Scheme 7. Use of Radical Trap X_2 To Quantify Cr(III)–R Homolysis


electron correlation problem is highly sensitive to ligand variation⁵³ and is notoriously difficult to model computationally.⁵⁴

Exploring Cr(III)–R Homolysis. With a series of Cr(III)–R compounds in hand we aimed to quantify the rate of homolysis of the Cr–C bonds. One challenge associated with monitoring the homolysis reactions is the buildup of the persistent radical trap Cr(II) throughout the reaction,⁵⁵ leading to a decrease in observed bond homolysis, by the equilibrium shown in Scheme 1. The bond dissociation energy for M–R can be determined using a radical trap that only reacts with R• if the trapping reactions are performed in the presence of excess reduced metal complex M.^{2a} Alternatively, k values for the bond homolysis can be obtained using a radical trap, X_2 , that consumes *both* the organic radical and the reduced metal complex (Scheme 7).²⁰

After consideration of alternative radical traps (see Supporting Information), PhSSPh was chosen as the X_2 source. PhSSPh serves as an effective single electron oxidant for Cr(II) and other organochromium species.⁵⁶ Reaction of CpCr[(XylNCMe)₂CH] with 0.5 equiv of PhSSPh in toluene provided the Cr(III)–SPh compound **15** (Figure 9). Alkyl radicals react with PhSSPh with $k = 1.7 \times 10^5 \text{ M}^{-1} \text{ s}^{-1}$,⁵⁷ and treating a $1 \times 10^{-4} \text{ M}$ solution of CpCr[(XylNCMe)₂CH] with 6 equiv of PhSSPh had quantitatively converted the Cr(II) to the Cr(III)–SPh **15** in the time (~3 min) required to transfer the cell from the glovebox to the UV–vis spectrophotometer. Compound **15** also has a minimum absorbance in the UV–vis at 560 nm, where the Cr(III)–R compounds absorb strongly (Figure 8), allowing relatively low concentrations of Cr(III)–R to be used in homolysis studies while still achieving large changes in absorbance and being able to stay within solubility limits of PhSSPh and compound **15** in hexanes solutions.

The Cr(III)–CH₂Ph compound **10** was found to react cleanly with 10 equiv of PhSSPh to give a first-order observed rate constant. Saturation kinetics were observed with a sufficient increase in the PhSSPh concentration allowing for the deter-

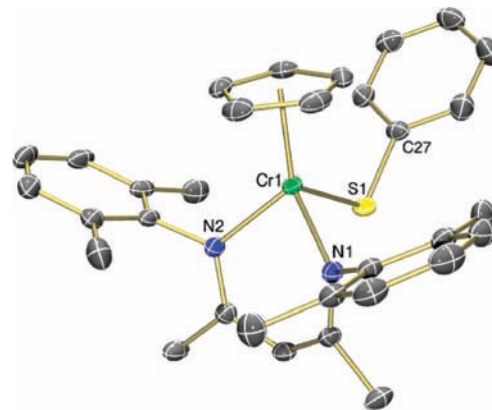


Figure 9. Thermal ellipsoid diagram (50%) of **15**. All H atoms are omitted for clarity.

Table 2. Comparison of Rate Constants for CpCr[(ArNCMe)₂CH]R Bond Homolysis

	Ar	R	Rate constant k (s ⁻¹)
2	Xyl	CH ₂ CMe ₃	$3.6(3) \times 10^{-3}$
7	Xyl	CH ₂ CHMe ₂	$\sim 1 \times 10^{-5}$
7a	Dpp	CH ₂ CHMe ₂	$\sim 5 \times 10^{-5}$
10	Xyl	CH ₂ Ph	$3.2(5) \times 10^{-3}$
10a	Dpp	CH ₂ Ph	$9(2) \times 10^{-3}$
10b	Dep	CH ₂ Ph	$1.1(7) \times 10^{-2}$
10c	Mes	CH ₂ Ph	$3.2(4) \times 10^{-3}$
11	Xyl	CH ₂ C ₆ H ₄ Me	$7.8(7) \times 10^{-3}$

mination of the rate constant ($k = 3.2(5) \times 10^{-3} \text{ s}^{-1}$) for the bond homolysis of **10** at room temperature. A list of rate constants for bond homolysis of Cr(III)–R compounds is given in Table 2.

Primary Cr(III)–R pentaqua complexes lacking stabilizing substituents are not generally observed to generate R• radicals.⁴⁸ However, neopentyl compounds of the first row transition metals have previously been reported to be particularly prone to M–R homolysis.⁵⁸ The observed rate constant for CpCr[(XylNCMe)₂CH](CH₂CMe₃) is consistent with the efficacy of **2** as an initiator for the OMRP of vinyl acetate.¹⁶ The dramatic decrease from $3.6(3) \times 10^{-3} \text{ s}^{-1}$ to $\sim 1 \times 10^{-5} \text{ s}^{-1}$ upon changing the alkyl group from neopentyl **2** to isobutyl **7** attests to the steric discrimination of CpCr[(XylNCMe)₂CH].

The dissociation constant of $3.2(5) \times 10^{-3} \text{ s}^{-1}$ measured for benzyl complex **10** is comparable to the value of $2.6(2) \times 10^{-3} \text{ s}^{-1}$ determined for [(H₂O)₅Cr(CH₂Ph)]²⁺ in aqueous solution.⁵⁹ It is also very close to that of neopentyl compound **2**. Despite this favorable dissociation rate, the relative stability of the benzyl radical makes **10** a less appealing reagent than **2** for OMRP: the rate constant for the reaction of PhCH₂• with vinyl acetate is $15 \text{ M}^{-1} \text{ s}^{-1}$, compared to $1.4 \times 10^4 \text{ M}^{-1} \text{ s}^{-1}$ for CH₃• with vinyl acetate.⁶⁰ Electronic effects on the rate of homolysis were also evident when comparing the benzyl compound (**10**) to the *para*-methylbenzyl compound (**11**), exhibiting a 2-fold increase in the rate constant with the introduction of a *p*-methyl substituent.⁵⁹ There was also a clear trend between the four

(53) (a) Nguyen, T.; Sutton, A. D.; Brynda, M.; Fetting, J. C.; Long, G. J.; Power, P. P. *Science* **2005**, *310*, 844–847. (b) Wolf, R.; Brynda, M.; Ni, C.; Long, G. J.; Power, P. P. *J. Am. Chem. Soc.* **2007**, *129*, 6076–6077. (c) La Macchia, G.; Li Manni, G.; Todorova, T. K.; Brynda, M.; Aquilante, F.; Roos, B. O.; Gagliardi, L. *Inorg. Chem.* **2010**, *49*, 5216–5222.

(54) (a) Hall, M. B. *Polyhedron* **1987**, *6*, 679–684. (b) Siegbahn, P. E. M. *Adv. Chem. Phys.* **1996**, *93*, 333–387.

(55) Daikh, B. E.; Finke, R. G. *J. Am. Chem. Soc.* **1992**, *114*, 2938–2943.

(56) Fryzuk, M. D.; Leznoff, D. B.; Rettig, S. J. *Organometallics* **1997**, *16*, 5116–5119, and references cited therein.

(57) Newcomb, M. *Tetrahedron* **1993**, *49*, 1151–1176.

(58) (a) Tsou, T. T.; Loots, M.; Halpern, J. *J. Am. Chem. Soc.* **1982**, *104*, 623–624. (b) Wayland, B. B.; Poszmik, G.; Mukerjee, S. L.; Fryd, M. *J. Am. Chem. Soc.* **1994**, *116*, 7943–7944. (c) Fernandez, I.; Trovitch, R. J.; Lobkovsky, E.; Chirik, P. J. *Organometallics* **2008**, *27*, 109–118.

(59) Nohr, R. S.; Espenson, J. H. *J. Am. Chem. Soc.* **1975**, *97*, 3392–3396.

(60) Fischer, H.; Radom, L. *Angew. Chem., Int. Ed.* **2001**, *40*, 1340–1371.

different β -diketiminato ligands when comparing the four Cr(III)–benzyl compounds (**10**–**10c**). The Xyl and Mes derivatives had the same rate constants indicating that there was no effect of the *para*-methyl groups of the Mes ligand compared to the Xyl ligand. There was, however, a clear trend in the steric profile of the ligands, with the bulkier Dep and Dpp ligands showing a 3-fold increase in the rate constant.

Compounds **1**, **4**, **5**, **8**, **9**, **12**, **13**, and **14** were all subjected to the same reaction conditions but were found to be stable with respect to bond homolysis. When the stock solution from the kinetic experiment with compound **4** was left to stand at ambient conditions in the glovebox, it did however react with the PhSSPh, to provide the expected Cr(III)–SPh compound (**15**), while the sample in the light-protected spectrophotometer remained unchanged. When the sample from the instrument was later removed and left to stand in ambient laboratory light it cleanly converted to **15** (UV–vis). Further experimentation revealed that all of the CpCr[(ArNCMe)₂CH](R) compounds except **14** are also cleanly converted to **15** when exposed to fluorescent lab light or sunlight in the presence of excess PhSSPh.

Reactivity Consequences of Cr(III)–R Photolysis. Photolysis is a well-known method to induce M–R bond homolysis,^{2b} and the photochemistry and photophysics of octahedral Cr(III) coordination complexes have been very well-studied.⁶¹ Nevertheless, the photolytic reactivity with PhSSPh was somewhat surprising since *under typical anaerobic conditions the CpCr[(ArNCMe)₂CH](R) complexes display no indication of being light sensitive.* Most of the Cr(III) alkyl compounds were synthesized in moderate to good yields despite the lack of any precautions to exclude light during their preparation, recrystallization, or subsequent handling. Solutions of the complexes prepared in the absence of PhSSPh remained unchanged by UV–vis after prolonged light exposure. Single crystal samples of the Cr(III) methyl compound **1b** suitable for X-ray diffraction that were stored under N₂ in a flame-sealed clear glass ampule were not visibly altered or degraded after direct exposure to ambient laboratory light for over 4 years.

The deceptive lack of apparent photolytic Cr–R homolysis is presumably due to the remarkable efficiency of CpCr[(XylNCMe)₂CH] as a trap for carbon-based radicals, allowing minute quantities of the Cr(II) complex to effectively preclude bimolecular R• reactions.²⁰ This reactivity mode only became apparent when the thermally stable CpCr[(XylNCMe)₂CH](R) compounds were exposed to light in the presence of excess PhSSPh, which consumes the Cr(II) trap as it is generated.

A 10^{−4} M solution of methyl complex **1** in hexanes with an excess of PhSSPh was exposed to light ≥ 500 nm in a fluorometer over a 30 min period with no change observed in the UV–vis spectrum. Upon exposure to light ≥ 400 nm compound **1** immediately began converting to **15**. The clean conversion of **1** to **15** was essentially complete after a total of 5 h of light exposure (kinetic trace available in the Supporting Information) over a 2 day period; after 94 min of light exposure the reaction was stored in the absence of light for 24 h giving identical UV–vis spectra before and after storage, demonstrating the need for a continual photon source to cause bond homolysis. This experiment indicated that the higher energy absorbance band (395–436 nm) in the UV–vis spectrum was responsible for bond homolysis.

As previously reported, the Cr(III)–Me compound **1** was not an efficient radical initiator for OMRP of vinyl acetate, giving 9% conversion over 48 h at room temperature when exposed to ambient lab light.¹⁶ When this experiment was repeated with the exclusion of light, no poly(vinyl acetate) was produced.

Perhaps the most significant consequence of the observed photolytic activity of the CpCr[(ArNCMe)₂CH](R) compounds is the connection with their sensitivity to air. The CpCr[(ArNCMe)₂CH] Cr(II) complexes are highly air sensitive as solids and in solution, as are the Cr(III) neopentyl and benzyl species. In contrast, the Cr(III) methyl and phenyl compounds are remarkably air stable in the absence of light. Notably, a 10^{−4} M solution of **1** in hexanes that was open to air was monitored by UV–vis in the dark for a 3 h period with no appreciable change in the spectra. In contrast, a similar solution of **10** decomposes within minutes upon air exposure in the dark. In the absence of light, the intact Cr(III) CpCr[(ArNCMe)₂CH](R) complexes do not apparently undergo outersphere oxidation with O₂. However, after photolytic Cr–R homolysis, the O₂ reacts very rapidly with both R• and the Cr(II) product. The similarity in the photolytic reactivity trends for the Cr(III)–R complexes using either PhSSPh or O₂ as the radical trap is consistent with the mechanism shown in Scheme 7. The Cr(III) phenyl complex **12** is relatively air stable as a solid under ambient lab light, consistent with the known stability of rigorously octahedral Cr(III) phenyl compounds bearing chelating ligands that do not readily dissociate to reactive five-coordinate intermediates.⁶²

Conclusions

Synthetic routes to CpCr[(ArNCMe)₂CH](R) complexes have been described from the corresponding Cr(III) chloride, tosylate, or triflate precursors. Rate constants for Cr–R bond homolysis were obtained by monitoring the reaction of the Cr(III) alkyls with excess PhSSPh by UV–vis spectroscopy. Modifying the neopentyl ligand from the previously reported CpCr[(XylNCMe)₂CH]–(CH₂CMe₃) complex **2** decreases its reactivity: replacing even one Me group with a H diminishes the rate of alkyl dissociation, while use of the CH₂SiMe₃ group effectively shuts down the thermal homolysis reaction at room temp. The rates for Cr–CH₂Ph homolysis are comparable to those for **2**, even though the benzyl complexes are much easier to prepare and handle than the reactive neopentyl compounds. The homolysis rates increased when bulkier Dpp and Dep substituents were used on the β -diketiminato ligands, consistent with the importance of steric repulsion in weakening the Cr(III)–R bonds.

The remaining CpCr[(ArNCMe)₂CH](R) complexes displayed unexpected Cr–R homolysis reactivity when exposed to ambient light in the presence of a reagent capable of consuming both R• and the Cr(II) products, such as PhSSPh or O₂. These well-defined Cr(III) compounds can thus generate hydrocarbyl radicals with a range of inherent reactivity under mild thermal or photolytic conditions. We are currently exploring the controlled generation of R• radicals from CpCr[(ArNCMe)₂CH]–

(61) Kirk, A. D. *Chem. Rev.* **1999**, *99*, 1607–1640.

(62) (a) Daly, J. J.; Sanz, F.; Sneed, R. P. A.; Zeiss, H. H. *J. Chem. Soc., Dalton Trans.* **1973**, 73–76. (b) Sneed, R. P. A.; Zeiss, H. H. *J. Organomet. Chem.* **1973**, *47*, 125–131. (c) Cotton, F. A.; Mott, G. N. *Organometallics* **1982**, *1*, 38–43.

(R) species for intermolecular and intramolecular carbon–carbon bond forming reactions.

Experimental Section

The complete Experimental Section is found in the Supporting Information. Representative examples of the three procedures outlined in Scheme 3 are given below.

Method A. CpCr[(XylNCMe)₂CH](Cl) (266 mg, 0.581 mmol) was added to a Schlenk flask in an inert atmosphere glovebox, followed by the addition of Et₂O (20 mL). ClMgCH₂CHMe₂ (0.32 mL of 2.0 M solution in Et₂O, 0.64 mmol, 1.1 equiv) was added dropwise to the stirring solution. The reaction mixture was stirred overnight at room temperature in the dark, and 1,4-dioxane (400 μL) was then added and stirred for 0.5 h at which point the solvent was removed *in vacuo*. The residue was extracted with hexanes (20 mL), filtered through Celite, and rinsed with hexanes (3 × 5 mL). The purple solution was concentrated to 15 mL, filtered, and cooled to –35 °C to yield crystals of **7** (179 mg, 64%) over several days in three crops. Anal. Calcd for C₃₀H₃₉N₂Cr: C, 75.12; H, 8.20; N, 5.84. Found: C, 74.87; H, 7.92; N, 5.86. UV/vis (hexanes; λ_{max}, nm (ε, M⁻¹cm⁻¹)): 396 (5510), 556 (1630).

Method B. Compound **3** (202 mg, 0.340 mmol) was added to a Schlenk flask in an inert atmosphere glovebox, followed by the addition of Et₂O (18 mL). Mg(CH₂SiMe₃)₂ · 1.05(1,4-dioxane) (54.6 mg, 0.188 mmol, 0.552 equiv) in Et₂O (4 mL) was added dropwise to the Schlenk flask. The reaction mixture was stirred overnight at room temperature, the solvent was removed *in vacuo*, the residue was extracted with hexanes and filtered through Celite, and the solvent was again removed *in vacuo*. The violet solid was extracted with a minimum amount of hexanes (4 mL), filtered, and cooled to –35 °C to yield black crystals of **4** (150 mg, 86%) over several days in two crops. Anal. Calcd for C₃₀H₄₁N₂SiCr: C, 70.69; H, 8.11;

N, 5.50. Found: C, 71.06; H, 8.11; N, 5.22. UV/vis (hexanes; λ_{max}, nm (ε, M⁻¹cm⁻¹)): 412 (6350), 568 (1180).

Method C. CpCr[(XylNCMe)₂CH] (102 mg, 0.241 mmol) was added to a Schlenk flask in an inert atmosphere glovebox, followed by the addition of THF (10 mL). ICH₂SiMe₃ (53.0 μL, 0.357 mmol, 1.49 equiv) was added to the solution and stirred for 10 min followed by the addition of Mn powder (133 mg, 2.42 mmol, 10 equiv). The reaction mixture was stirred for 24 h at room temperature, at which point the reaction was determined to be complete by UV–vis spectroscopy. The reaction mixture was then stirred for an additional 24 h, and the solvent was removed *in vacuo*. The residue was extracted with hexanes (10 mL), filtered through Celite, and rinsed with hexanes (3 × 5 mL). The violet solution was concentrated to 3 mL and cooled to –35 °C to yield crystals of **4** (89.4 mg, 73%) over several days in two crops, purity confirmed by UV–vis spectroscopy.

Acknowledgment. We are grateful to the Natural Sciences and Engineering Research Council of Canada (NSERC), the Canadian Foundation for Innovation, and the University of British Columbia for financial support. K.M.S. thanks Katherine H. D. Ballem (UPEI) for the synthesis of complex **6a'** and Dr. James Bailey for assistance with the fluorometer photolysis kinetic measurements.

Supporting Information Available: Complete experimental details, UV–visible spectra, and crystallographic data for complexes **2c**, **3b**, **3c**, **4**, **4a**, **4b**, **4c**, **5**, **6'**, **6a'**, **7**, **7a**, **8**, **9**, **10**, **10a**, **10b**, **10c**, **11**, **12**, **13**, **14**, and **15**. This material is available free of charge via the Internet at <http://pubs.acs.org>.

JA1083392